วารสารวิชาการวิศวกรรมศาสตร์ ม.อบ.
UBU Engineering Journal

บทความวิจัย

Adsorption of Reactive Red 120 onto Cationic Surfactant Intercalated Montmorillonite Clay

Pariwat Namdaung[1] Chakkrit Umpuch[1]*

[1] Department of Chemical Engineering, Faculty of Engineering, Ubon Ratchathani University, Warin Chamrap, Ubon Ratchathani 34190

*Corresponding author.

E-mail: chakkrit.u@ubu.ac.th; Telephone: 0 4535 3361.

Received 5 July 2018; Revised #1 10 October 2018; Revised #2 2 January 2019; Accepted 1 January 2019.

Abstract

In this work, cationic surfactant intercalated-montmorillonite (OMt) was prepared as adsorbent used for the removal of Reactive Red 120 (RR120) from aqueous solutions. The OMt and as received motmorillonite (Mt) were characterized by the FTIR, BET method, SEM, and XRD. The affecting factors such as contact time, initial dye concentration, initial pH, and temperature were investigated. The result revealed that adsorption of RR120 reached equilibrium at 480 minutes. The uptake of RR120 increased with temperatures, indicating an endothermic process. The adsorption capacity was slightly decreased with increasing in pH. Kinetics data were well described by the pseudo-second order model. The equilibrium data were better fitted by the Langmuir isotherm and the maximum monolayer adsorption capacity was 268.54 mg. g^{-1}. These results suggested that the OMt is an effective adsorbent for removing RR120 from aqueous solutions.

Keywords

adsorption; reactive red 120; cationic surfactant; montmorillonite clay.

1. Introduction

Reactive dyes are most commonly used as colorants in textile industry because of the durability of bleaching and high stability with the fibers. However, in the dyeing process, 10–50% of dye used was hydrolyzed and lost through the effluent [1]. Furthermore, the well-known azo bond (N=N) in their structure make them tolerance to degradation by conventional biological treatment, giving them a high chance to contaminating the water body. The release of colored water into the natural stream harms the aquatic life though photosynthetic activity reduction, and toxicity due to potential groups such as aromatic amines [2].

Of the several methods of dyes removal from wastewater such as chemi-coagulation, membrane separation, oxidation, and electro-coagulation, adsorption has been proven to be an effective and easily applied method. It is an accumulation of target substances (adsorbates) onto a solid surface

(adsorbents) by physico-chemical interactions without the generation of any harmful by-products during the treatment process. However, the adsorbent itself can be costly and hard to regenerate, making alternative low-cost adsorbents interesting.

Montmorillonite (Mt) has been accepted as one of the low-cost adsorbents [3,4]. In Thailand, Mt is very cheap and commercially produced. It is a member of the smectite group, a 2:1 clay having 2 tetrahedral sheets sandwiching a central octahedral sheet in which Al^{3+} is isomorphously substituted with Mg^{2+} resulting in its permanently negatively charge surface. The interlayer spaces are also expandable according to adsorbed molecules. Referring to a study by Monvisade and Siriphannon [5], cationic dyes with different molecular diameters can be adsorbed by Mt, the smaller dye had greater capacity. However, Reactive Red 120 (RR120) was used as a representative of anionic reactive dye. A preliminary study by the authors of the present research showed poor results (%Dye removal <5%), which may be due to (1) the repulsive force between the negatively fixed charge on the Mt surface and the RR120 anions, and (2) the large molecular diameter of RR120.

To overcome this problem, many modifications of Mt by various substances to alter its surface properties and increase the interlayer space were reported [6]. Mt modified by many kinds of surfactants were successful in adsorbing organic substances such dyes [7,8], antibiotics [9], herbicides [10], and phenolic compounds [10]. These modifications focused on adding hydrophobic parts and favorable active sites on to Mt.

In this work, the Mt and one modifying with a cationic surfactant, cetyltrimetyl ammonium bromide (CTAB), called “cationic surfactant intercalated montmorillonite (OMt)”, were used as the adsorbents. The adsorbents were characterized using FT-IR, BET-method, SEM, and XRD. The schematic diagram of the OMt was illustrated. Batch adsorptions were tested with RR120 to study the isotherms, kinetics, and effect of pH and temperature.

2. Materials and Methods

2.1 Chemicals

Montmorillonite clay (Mt) was supplied by Thai Nippon Chemical Industry Co. Ltd., Thailand, had a cation exchange capacity (CEC) of 0.8 meq.g^{-1}. Reactive Red 120 (RR120), and cetyltrimethyl ammonium bromide (CTAB) were purchased from Sigma Aldrich, USA. All other chemicals were of analytical grade and used as received. pH was adjusted by NaOH or HCl solutions. All solutions were prepared and washed with distilled water.

2.2 Preparation of OMt

The amount of surfactant (CTAB) equivalent to 1.5 CEC of Mt was dissolved in 100 mL distilled water. 1.0 g of Mt was added into each of the mixtures and continuously agitated by a stirrer for 12.0 hr. The solid phases were separated and washed several times until the washed water reached constant conductivity. The product was dried in a hot air oven at 105 °C and ground through 200 mesh sieve. The

final product is called “cationic surfactant intercalated-montmorillonite (OMt)”.

2.3 Characterization of the adsorbents

The functional groups of the adsorbents were analyzed with Perkin Elmer Spectrum Two ATR-FTIR spectrometer. The morphologies were observed with a JSM-5410LV SEM, at 20 kV and 10,000X magnification. The specific surface areas and pore sizes were analyzed by BET method using nitrogen adsorption-desorption isotherm with Automatic Surface Analyzer. The interlayer spaces were analyzed with X-ray fluorescence spectrometer with CuK α-radiation λ = 1.542 Å at 40 kV with 20 mA. All XRD patterns, the 2θ were varied from 5° to 16° with a scan 2θ speed of 0.02 °.min^{-1}.

2.4 Adsorption studies

RR120 was dissolved to 1,000 mg.L^{-1} as stock solution. The adsorption tests were performed in an incubator shaker with desired temperatures and 200 rpm. Preliminary studies showed that the dye adsorption was completed within 8.0 hr. The dye concentrations were analyzed at 534 nm by an UV/Visible spectrometer. The amount of RR120 adsorbed on the adsorbents, qt, was obtained as follows:

$$qt = (C_0 - C_t)V/W \quad (1)$$

where C_0 and C_t are the concentration of RR120 at initial and any time t (mg.L^{-1}), respectively, V is the volume of solution (L) and W is the amount of adsorbent (g).

For kinetics studied, twelve Erlenmeyer flasks of 100 mL 300 mg.L^{-1} dye solution and 0.1 g adsorbent were shaken at 35 °C. In the pre-determined time intervals, the dye concentrations in each flask were measured. The adsorbents were separated from the suspension by a centrifuge at 8,000 rpm for 5 min. For isotherm studies, 100 mL dye solutions ranging from 50 to 300 mg.L^{-1} were pour in the flasks. Then, 0.1 g adsorbent was added and shaken at 35 °C. The mixtures were left over night to ensure equilibrium. Then the adsorbent was removed and the supernatant was measured for dye concentration. To study effects of temperature, similar procedures to kinetic and isotherm studies were performed at 45, 55, and 65 °C. The influence of pH on the adsorption was tested with different initial pH (2 to 10) of 100 mL 300 mg.L^{-1} dye solution at 35 °C. When the equilibrium was reached, the adsorbent was separated and the dye concentration was measured.

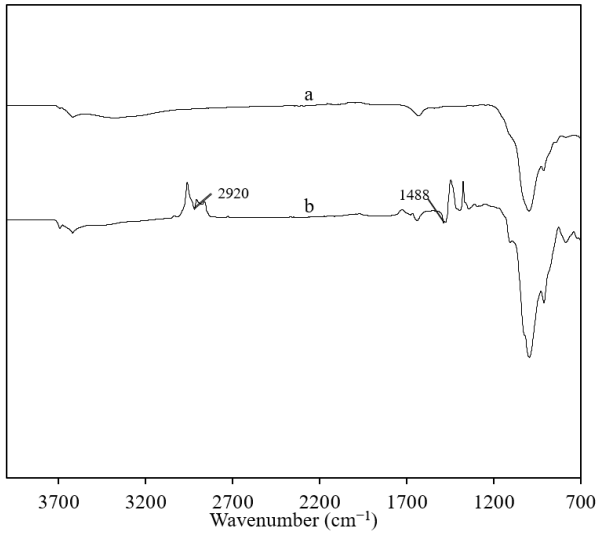

Fig. 1 IR spectrum of as received (a) Mt, and (b) OMt

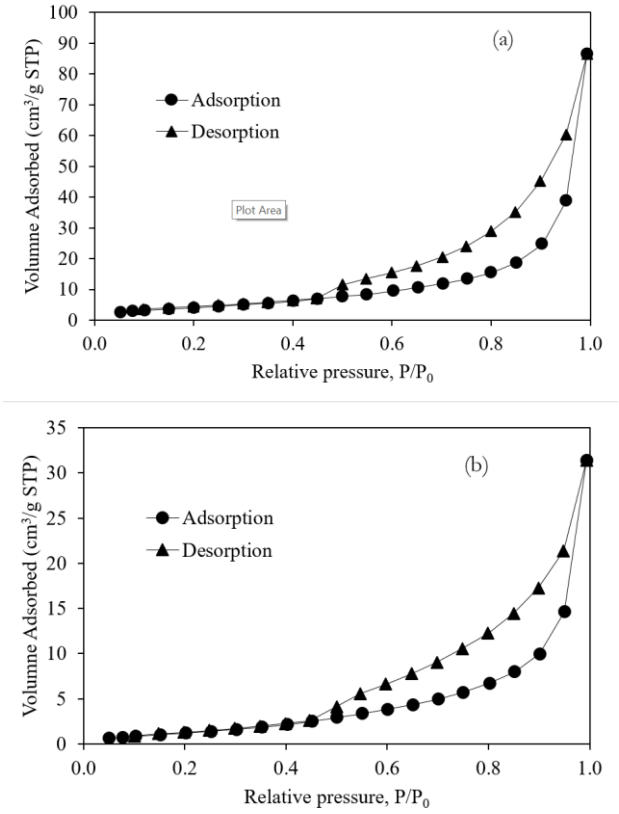

Fig. 2 N_2 adsorption–desorption isotherm of (a) Mt, and (b) OMt

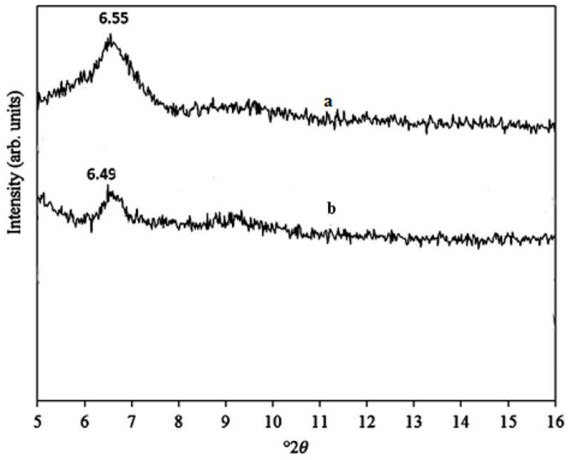

Fig. 3 XRD powder patterns of (a) Mt and (b) OMt

3. Results and Discussions

3.1 Adsorbent characterizations

The FTIR spectrums (Fig. 1) show obvious changes after the modifications. The IR spectrum of Mt was shown in Fig.1a. The modifications show the band at 2,945 to 2,879 cm^{-1} corresponding to the C-H stretching which was present in surfactant molecules. The band at 1488 cm^{-1} indicated the C-H bending of the alkyl chain was presented (Fig. 1b). The results showed that the modifications were successful in attaching the modified reagents into Mt [11].

Table 1 Specific surface areas, specific pore volumes, and average pore diameters of the adsorbents.

Parameter	Mt	OMt
Specific surface area (m^2/g)	54.17	6.94
Total pore volume (mL/g)	0.17	0.073
Average pore size (nm)	1.26	4.22
d-spacing (nm)	1.35	3.79

In Fig. 2, all the adsorbents show type IV isotherm according to IUPAC classification indicating mesoporous structures. However, the BET average pore sizes (Table 1) of Mt is in range of microporous (>2 nm, IUPAC standard), therefore the hysteresis loops occurred were considered as a slits pore shape. The increases in pore sizes of modified Mt was an evidence of intercalation of modified reagent. The inter-lamellar of Mt expands when cationic species intercalate. It acts as a pillar keeping the aluminosilicate sheets permanently apart. The decreases in BET specific surface area of all modified Mt may have two possible explanations. First, the modified reagent covered up the roughness on the Mt surface directly reducing it. Second, they packed very compactly, blocking the nitrogen molecules to get into the interior area of the Mt [12].

In Fig. 3, the peak for Mt was observed at 2θ = 6.55°. The modification of Mt with CTAB caused the

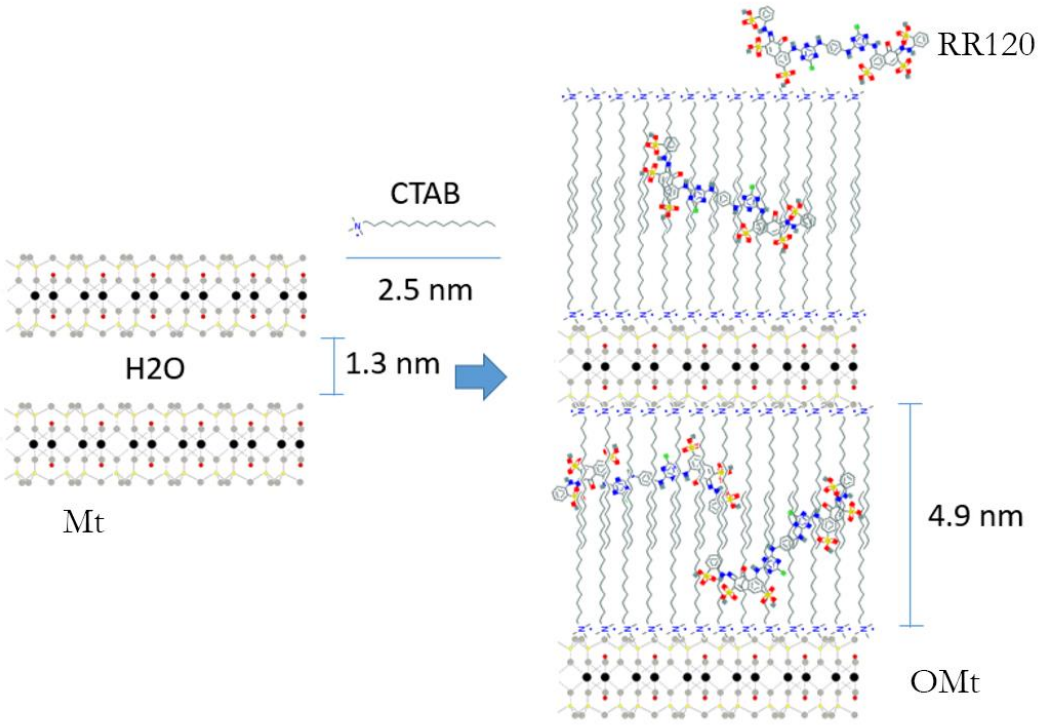

Fig. 4 Expansion of interlayer spacing due to the adsolubilization of Mt with CTAB

diffraction peak of Mt shifting to a new peak at 2θ = 6.49°. The values of d-spacing of Mt and OMt were 13.5 Å and 37.9 Å, respectively. The Shifting of the diffraction peak to a lower angle referred to an increase of d-spacing [13]. The enlargement of interlayer of Mt after modification was illustrated in Fig.4. The surfactant transferred to the external surface of Mt. Then admicelle was formed and covered up the external surface. In addition, some of them entered into the interior of Mt and formed pillared like structure. The observed results were similar to that in previous literatures [14].

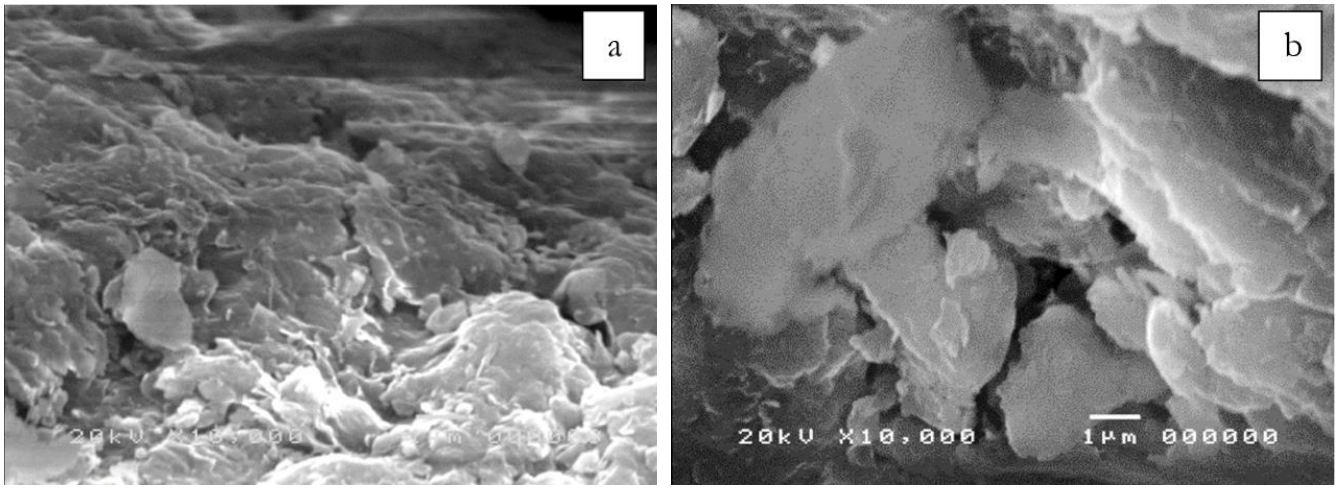

Fig. 5 SEM images of as received (a) Mt and (b) OMt

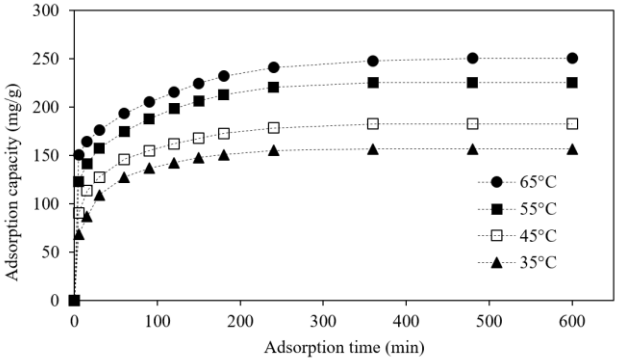

Fig. 6 Adsorption kinetic for the adsorption of RR120 on OMt, Initial RR120 concentration: 300 $mg.L^{-1}$

After modifications, the small particles of the Mt (Fig. 5a) were covered up with CTAB and became larger flask-like particles (Fig. 5b). These particles piled up into multi-layers leading to cavity-like structure, which were convenient for the dye molecules to diffuse into the interior structures.

3.2 Effect of contact time

After finishing the modification, the adsorbent (OMt) was obtained and tested for percent of dye removal. The percent dye removal of OMt was 100%, which was much higher that of the Mt (0%). In the case of OMt, the dye molecules were induced by fixed positive charged on the external surface of the admicelle and then adsorbed into the admicelle body.

In Fig. 6, the adsorption capacity increased rapidly at first 30 minutes and then slowly increased until it reached constant, which is assigned as equilibrium stage. Under the experimental conditions, the equilibrium time for the adsorption of RR120 on OMt is 480 minutes. The results showed that at the initial stage, a large amount of dye molecules were adsorbed onto the available active sites at the external surface of admicelle, which is rapidly and then slowly diffused into the interior spaces of the adsorbent. Eventually, the available sites are fully occupied causing constant adsorption capacity at the equilibrium time.

3.3 Effect of initial dye concentration

The driving forces due to the initial dye concentration gradient are an important factor for dye molecules to overcome the mass transfer resistances between the aqueous and solid phases. The RR120 uptakes increase from 42.06 to 115.99 $mg.g^{-1}$ with increased the initial dye concentrations from 50 to 150 $mg.L^{-1}$ and then slightly increases from 115.99 to 148.75 $mg.g^{-1}$ when initial concentrations increase from 150 to 300 $mg.L^{-1}$. At low initial dye concentration, the adsorption capacity was low due to insufficient driving force for dye molecules to overcome the mass transfer resistances leading to unsaturated active sites on the adsorbent. At higher initial dye concentrations, the dye molecules have greater driving force, thus more active sites occupied.

3.4 Effect of temperature

The amount of RR120 adsorbed on OMt increased from 148.75 to 185.36, 230.45, and 245.91 $mg.g^{-1}$ with increases in operating temperatures from 35 to 45, 55, and 65°C respectively (See Table 2). It was found that the increase of temperature facilitates the adsorption capacity indicating a nature endothermic process. This increase of temperature may cause swelling effect expanding the basal spacing inside the internal

Table 2 Results of Isotherm parameters for the adsorption of RR120 onto OMt

Parameters	Temperature (°C)			
	35	45	55	65
q_{exp} (mg. g^{-1})	148.75	185.36	230.46	248.95
Langmuir isotherm				
q_m(mg. g^{-1})	162.60	199.21	250.67	265.00
b (L. mg^{-1})	0.2179	0.0635	0.1164	0.1333
R^2	0.9992	0.9979	0.9987	0.9991
R_L	0.2396	0.1466	0.1304	0.0841
Freundlich isotherm				
n	2.7639	2.7881	2.5405	2.5484
K_f (mg. g^{-1})	26.8903	40.0011	48.6147	61.8833
R^2	0.9013	0.8942	0.9521	0.9187

structure of adsorbent and allowing higher amount of dye molecules to penetrate into the wider internal space. The similar pore size enlarging effect and endothermic process were also observed in other works such as the adsorption of reactive dyes on activated carbon and Fe_3O_4 magnetic nanoparticles [15,16].

3.5 Effect of initial pH

In Fig. 7, it can be seen that the adsorption capacity slightly decreased from 163.60 to 144.46 mg.g^{-1} when the pH was increased from 2 to 10. In acidic condition, the dyes preferred to stay in the acid form increasing their hydrophobicity and made them easier to get adsorbed into the admicelle. Although, the surfactant modification can reduce the repulsive forces of Mt negative charged surface, slightly negative charge could be observed [17]. Therefore, increase of dissociate dye molecule along with pH

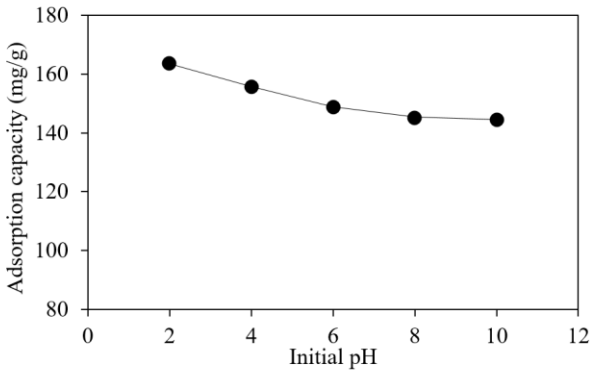

Fig. 7 Effect of initial pH on the adsorption capacities of OMt, Initial RR120 concentration: 300 mg.L^{-1}

makes repulsive force between dye and adsorbent stronger, resulting in decreased adsorption capacity. The diffusion coefficient of the dyes increased with pH made dyes molecules likely to stay in aqueous solution [17]. However, relatively high adsorption capacity revealed that the major interactive force came from hydrophobic interaction.

3.6 Adsorption isotherms

Fig. 8 shows adsorption isotherm, which is a plot of adsorption capacity versus equilibrium dye concentration. It can be seen that adsorption capacity significantly increases at low equilibrium dye concentration and then increases gradually at higher equilibrium dye concentration. The equilibrium data at different temperatures are interpreted using Langmuir and Freundlich adsorption isotherm models.

The Langmuir model was developed based on the assumption of the formation of monolayer adsorption and the surface is energetically homogeneous [18]. Linear form of the rearranged Langmuir model is

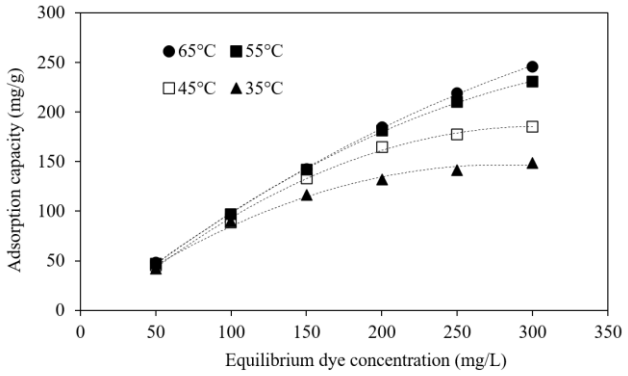

Fig. 8 Adsorption isotherm for the adsorption of RR120 on OMt, Adsorbent concentration: 0.1 g/100ml, pH 5.5±0.4, adsorption time: 12.0 h

$$C_e/q_e = 1/bq_m + C_e/q_m \quad (2)$$

where q_e is the amount of dye adsorbed at equilibrium (mg.g^{-1}), C_e is the dye concentration in solution at equilibrium (mg.L^{-1}), q_m is a constant related to maximum adsorption capacity (mg.g^{-1}) at equilibrium and b is Langmuir constant related to energy of adsorption (L.mg^{-1}).

The constants q_m and b can be calculated from the slope and intercept of the plot of C_e/q_e versus Ce and results are presented in Table 2. The Langmuir monolayer maximum adsorption capacity (q_m) increased from 162.60 to 265.00 mg.g^{-1} while increasing the temperature from 35 to 65 ℃.

The essential characteristics of Langmuir isotherm can be expressed by dimensionless constant called equilibrium parameter, R_L .

$$R_L = 1/(1 + bC_0) \quad (3)$$

where b is the Langmuir constant and C_0 is the initial concentration (mg.L^{-1}).

The value of R_L indicates the nature of the adsorption process as unfavorable ($R_L > 1$), linear ($R_L = 1$), favorable ($0 < R_L < 1$), and irreversible ($R_L = 0$). In the results from Table 2, the R_L value ranges between zero and one for the range of temperatures studied indicate that the adsorption is favorable.

The Freundlich model is usually adopted for heterogeneous adsorption. One of its limitations is that the amount of adsorbed solute increases indefinitely with the concentration of solute in the solution [19]. The linear form of this isotherm can be described as:

$$\ln q_e = \ln K_f + (1/n)\ln C_e \quad (4)$$

where K_f (mg.g^{-1}) is the measure of adsorption capacity and n is the adsorption intensity.

For the intensity parameter, $1/n$ indicates the deviation of the adsorption isotherm from linearity. n = 1 indicates the adsorption is linear with homogeneous adsorption sites and there is no interaction between the adsorbed molecules. $1/n$ <1 shows that the adsorption is favorable, new adsorption sites are available, and the adsorption capacity increases. $1/n$ > 1 indicates that the adsorption bonds are weak, and adsorption capacities decrease and are unfavorable.

A plot of ln q_e versus log C_e gives a linear line with a slope of $1/n$ and intercept of ln K_f , and results are presented in Table 2. The Freundlich constants are reported in Table 2, K_f increases from 26.89 to 61.88 mg. g^{-1} with increasing in temperature.

The value of n varies from 2.76 to 2.54 indicating that the adsorption of RR120 onto OMt is favorable.

However, both Freundlich and Langmuir models could describe the nature of adsorption with the experimental conditions because of good correlation coefficients.

3.7 Adsorption kinetics

Adsorption is a multi-steps process. To understand the adsorption mechanisms of RR120 on the adsorbents, pseudo-first-order and pseudo-second-order kinetic models are used.

The pseudo-first-order equation proposed by Lagergren [20] is similar to diffusion rate equation indicating the rate of limiting step is the diffusion of dye molecules through the boundary film. The integrated form this model can be expressed as:

$$\ln\left(q_e - q_t\right) = \ln\left(q_e\right) - k_1 t \qquad (5)$$

where q_e and q_t (mg.g^{-1}) are the amount of dye adsorbed at equilibrium and at time t (min) respectively, and k_1 (min^{-1}) is the rate constant of the pseudo-first order equation.

The pseudo-first order kinetic results are given in Table 3. The calculated equilibrium sorption capacity q_e (cal) and the q_e (exp) values show large deviations. The pseudo first-order rate law fails to explain the adsorption of RR120 by OMt with poor fit as the correlation coefficient ranged between 0.9402 and 0.9608.

The pseudo-second-order model is based on the assumption of chemisorption of the adsorbate on the adsorbents [21]. Its linearized form is given as:

Table 3 Results of kinetic modelling for the adsorption of RR120 onto OMt.

Parameters	Temperature (°C)			
	35	45	55	65
$q_{e(exp)}$ (mg. g^{-1})	156.48	182.41	225.00	250.46
Pseudo-first-order model				
k_1 (min^{-1})	0.00613	0.00539	0.00532	0.00466
$q_{e(cal)}$ (mg. g^{-1})	83.17	99.46	127.61	125.56
R^2	0.9456	0.9608	0.9402	0.9601
Pseudo-second-order model				
$k_2 \times 10^3$ (g. mg^{-1}. min^{-1})	0.5724	0.4898	0.3812	0.3563
$q_{e(cal)}$ (mg. g^{-1})	160.00	184.84	228.31	250.00
R^2	0.9982	0.9970	0.9939	0.9960

$$t/q_t = 1/\left(k_2 q_e^{\,2}\right) + t/q_e \qquad (6)$$

where k_2 is the equilibrium rate constant of the pseudo-second order equation (g.mg^{-1}.min^{-1}).

A plot of t/q_t and t should give a linear relationship if the adsorption follows second order equation. The q_e and k_2 can be calculated from the slope and intercept of the plot. The pseudo-second-order results are given in Table 3. The equilibrium sorption capacity q_e (cal) and q_e (exp) are very much similar to the experimental data. From the results, it is clear that equilibrium sorption capacity q_e increases with increases in temperature. However, the pseudo second-order rate constant k_2 decreases with increases the temperature. These results indicated that at higher temperature the equilibrium trends to reach slower but greater in capacity. The adsorption of RR120 by OMt is explained well by pseudo-second order kinetics with a very high

correlation coefficient of 0.9939 < R^2 < 0.9982, indicated that the formation rate of adsorbate and adsorbent interaction on the external surface of adsorbent is the rate of limiting step.

3.8 Thermodynamics parameters

The activation energy for the adsorption of RR120 onto OMt is evaluated using the following form of Arrhenius equation.

$$\ln(k_2) = \ln A - E_a/RT \quad (7)$$

where k_2 (g.mg^{-1}.min^{-1}) is the pseudo second order rate constant, E_a (kJ.mol^{-1}) is the Arrhenius activation energy of adsorption and A is the Arrhenius factor, R is the gas constant which is equal to 8.314 J.mol^{-1}.K^{-1}, and T (K) is the system temperature.

E_a and the A can be calculated from slope and intercept of the plot of ln k_2 vs $1/T$. It was found that the E_a obtained for the adsorption of RR120 by OMt was -14.52 kJ.mol^{-1}. The negative sign of E_a meant that there was no energy required for the reaction process, which was related to physisorption [22].

The other thermodynamic parameters such as Gibbs free energy change (ΔG°), standard enthalpy (ΔH°), and standard entropy (ΔS°) were calculated to identify the influence of temperature on the adsorption process using the following equations:

$$\Delta G^\circ = -RT \ln K_0 \quad (9)$$

$$\ln K_0 = \Delta H^\circ / RT + \Delta S^\circ / R \quad (10)$$

where K_0 is the Langmuir equilibrium constant, T is the solution temperature in Kelvin and R is a gas constant (8.314 J.mol^{-1}.K^{-1}).

Table 4 Thermodynamic parameters for the adsorption of RR120 onto OMt.

Temperature (°C)	ΔG° (kJ.mol^{-1})	ΔH° (kJ.mol^{-1})	ΔS° (J.mol^{-1}.K^{-1})
35	-7.06	33.25	85.50
45	-5.69		
55	-5.49		
65	-4.28		

The values of ΔH° and ΔS° were evaluated from the slope and intercept of van't Hoff plot [23] of ln K_0 vs $1/T$ and the results are presented in Table 4.

The negative standard Gibbs free energy change depicted the spontaneous nature of adsorption. However, the adsorption of RR120 by OMt was less favored by high temperature as indicated by the less negative Gibbs free energy (from -7.06 to -4.28 kJ.mol^{-1}) during the temperature increase. Standard enthalpy change ΔH° was 33.25 kJ.mol^{-1} (less than 80 kJ.mol^{-1}) and substantiated the physisorption and the positive sign indicated the endothermic nature of RR120 adsorption by OMt. The positive ΔS° (85.50 J.mol^{-1}.K^{-1}) indicating the randomness increased of the system by replacing the sorbed solvent molecules on adsorbent surface with the adsorbate molecules [24].

4. Conclusions

The OMt exhibited good adsorption capacity for removal of RR120 from aqueous solutions. The adsorption was affected by contact time, initial dye concentration, temperature, pH. The adsorption equilibrium was attained within 480 min and the

maximum adsorption was obtained at the initial solution pH of 2.0 and temperature at 65 °C. The equilibrium data obtained at different temperatures fitted well with the Langmuir model. The maximum monolayer capacity of RR120 adsorbed onto OMt increased from 148.75 to 245.91 $mg.g^{-1}$ with temperature increased from 35 to 65 °C, showing the uptake of RR120 increased with operating temperature. The calculated values of ΔH°, ΔS°, and ΔG° suggested that the adsorption was endothermic, random, and spontaneous. Regarding kinetic studies, the pseudo-second order kinetic model agreed with the dynamic behavior for the adsorption of RR120 onto OMt, with activation energy of -14.52 $kJ.mol^{-1}$. Though the results from kinetic experiments revealed the adsorption process is chemisorption, others support physisorption. Therefore, the adsorption process may involve both chemisorption and physisorption. These results suggested that OMt is a potential adsorbent for the reduction of the accumulation of dyes normally found in the effluent of various industries.

Acknowledgement

The Graduate Program in Environmental Engineering, Department of Chemical Engineering, Ubon Ratchathani University is gratefully acknowledged for the financial support. The authors express their sincere gratitude to staff of the Office of International Relations at Ubon Ratchathani University for assistance with English.

References

[1] Kant R. Textile dyeing industry an environmental hazard. *Natural science*. 2012.;4(1): 22–26.

[2] O'Neill C, Lopez A., Esteves S, Hawkes FR, Hawkes DL, Wilcox S. Azo-dye degradation in an anaerobic-aerobic treatment system operating on simulated textile effluent. *Microbiol. Biotechnol*. Appl. 2000; 53(2): 249–254.

[3] Umpuch C, Jutarat B. Adsorption behavior of reactive black 5 dye on activated carbon prepared from sugarcane bagasse. *UBU Eng. J*. 2012; 5(2): 10–21.

[4] Umpuch C. Modification of montmorillonite clay for dye removal from wastewater: a review. *UBU Eng. J*. 2012; 5(1): 56–66.

[5] Monvisade P, Siriphannon P. Chitosan intercalated montmorillonite: Preparation characterization and cationic dye adsorption. *Clay Sci*. Appl. 2009; 42 (3,4): 427–431.

[6] Zhang R, Yan W, Jing C. Mechanistic study of PFOS adsorption on kaolinite and montmorillonite. *Colloids and Surf. A*. 2014; 462: 252–258.

[7] Bhattacharyya R, Ray SK. Removal of congo red and methyl violet from water using nano clay filled composite hydrogels of poly acrylic acid and polyethylene glycol. *Chem. Eng. J*. 2015; 260: 269–283.

[8] Zhu L, Ma J. Simultaneous removal of acid dye and cationic surfactant from water by bentonite in one-step process. *Chem. Eng. J*. 2008; 139(3): 503–509.

[9] Meira SMM, Jardim AI, Brandelli A. Adsorption of nisin and pediocin on nanoclays. *Food Chemistry*. 2015; 188: 161–169.

[10] Rytwo G, Gonen Y, Afuta S, Dultz S. Interactions of pendimethalin with organo-montmorillonite complexes. *Appl. Clay Sci*. 2015; 28(1–4): 67–77.

[11] Anjaneyulu U, Swaroop V, Vijayalakshmi U. Preparation and characterization of novel Ag doped hydroxyapatite–Fe_3O_4 – chitosan hybrid composites and in vitro biological evaluations for orthopaedic applications. *RSC Advances*;2016: 6(13). 10997–11007.

[12] Wang CC, Juang LC, Hsu TC, Lee CK, Lee LF, Huang FC. Adsorption of basic dyes onto montmorillonite. *J. Colloid Interface Sci*. 2004; 273(1): 80–86.

[13] Myshakin EM, Wissam AS, Vyacheslav NR, Randall TC, Kenneth D. Molecular dynamics simulations of carbon dioxide intercalation in hydrated Na-montmorillonite. *J. Phys. Chem. C*. 2013; 117(21): 11028–11039.

[14] Zhou Q, Frost RL, He H, Xi Y. TEM, XRD, and thermal stability of adsorbed paranitrophenol on DDOAB organoclay. *J. Colloid Interface Sci*. 2007; 311(1): 24–37.

[15] Lorenc-Grabowska E, Gryglewicz G. Adsorption characteristics of Congo Red on coal-based mesoporous activated carbon. *Dyes Pigm*. 2007; 7(1): 34–40.

[16] Mittal H, Ballav N, Mishra S, Gum Ghatti. Fe_3O_4 magnetic nanoparticles-based nanocomposites for the effective adsorption of methylene blue from aqueous solution. *J. Ind. Eng. Chem*. 2014; 20: 2184–2192.

[17] Da Silva JS, Junqueira HC, Ferreira TL. Effect of pH and dye concentration on the n-octanol/water distribution ratio of phenothiazine dyes: a microelectrode voltammetry study. *Electrochim*. Acta. 2014; 144: 154–160.

[18] Langmuir I. The adsorption of gases on plane surfaces of glass, mica and platinum. *J. Am. Chem. Soc*. 1918; 40(9): 1361–1403.

[19] Umpuch C, Sakaew S. Removal of methyl orange from aqueous solutions by adsorption using chitosan intercalated montmorillonite. *Songklanakarin J. Sci*. Technol. 2013; 35(4): 451–459.

[20] Yuh-Shan H. Citation review of Lagergren kinetic rate equation on adsorption reactions. *Scientometrics*. 2004; 59(1): 171–177.

[21] Ho Y, McKay G. The kinetics of sorption of basic dyes from aqueous solution by sphagnum moss peat. *Can. J. Chem. Eng*. 1998; 76(4): 822–827.

[22] Kobiraj RN, Gupta AK, Kushwaha AK, Chattopadhyaya MC. Determination of equilibrium, kinetic and thermodynamic parameters for the adsorption of Brilliant Green dye from aqueous solutions onto eggshell powder. *Indian J. Chem*. Technol. 2012; 19: 26–31.

[23] Lyubchik, S, Perepichka I, Galushko O, Lyubchik A, Lygina E, Fonseca I. Optimization of the conditions for the Cr(III) adsorption on activated carbon. *Adsorption*. 2005; 11(5,6): 581–593.

[24] Maszkowska J, Wagil M, Mioduszewska K., Kumirska J, Stepnowski P, Biatk-Bielinska A. Thermodynamic studies for adsorption of ionizable pharmaceuticals onto soil. *Chemosphere*. 2014;111: 568–574.